

# <sup>1</sup> Functional MRI brain state <sup>2</sup> occupancy in the presence of <sup>3</sup> cerebral small vessel disease – <sup>4</sup> pre-registration for a multiverse

✉ For correspondence:

e.schlemm@uke.de

Present address:

Dr. Dr. Eckhard Schlemm,  
Klinik und Poliklinik für  
Neurologie,  
Universitätsklinikum  
Hamburg-Eppendorf,  
Martinistr. 52,  
D-20251 Hamburg

## <sup>5</sup> replication analysis of the Hamburg <sup>6</sup> City Health Study

<sup>7</sup> **Eckhard Schlemm, MBBS PhD**  

<sup>8</sup> <sup>1</sup>Department of Neurology, University Medical Center

<sup>9</sup> Hamburg-Eppendorf

Data availability:

Preprocessed data will be  
available e.g. on

<https://github.com/csi-hamburg/HCHS-brain-states-RR>.

Funding: Deutsche  
Forschungsgemeinschaft  
(DFG) - 178316478 - C2

Competing interests: The  
author declares no  
competing interests.

### <sup>11</sup> Abstract

<sup>12</sup> **Objective:** To replicate recent findings about the association between the extent of  
<sup>13</sup> cerebral small vessel disease (cSVD), functional brain network dedifferentiation and  
<sup>14</sup> cognitive impairment.

<sup>15</sup> **Methods:** We will analyze demographic, imaging and behavioral data from the  
<sup>16</sup> prospective population-based Hamburg City Health Study. Using a fully prespecified  
<sup>17</sup> analysis pipeline, we will estimate discrete brain states from structural and resting-state  
<sup>18</sup> functional magnetic resonance imaging (MRI). In a multiverse analysis we will vary brain  
<sup>19</sup> parcellations and functional MRI confound regression strategies. Severity of cSVD will

<sup>20</sup> be operationalised as the volume of white matter hyperintensities of presumed  
<sup>21</sup> vascular origin. Processing speed and executive dysfunction are quantified by the trail  
<sup>22</sup> making test (TMT).  
<sup>23</sup> **Hypotheses:** We hypothesize a) that greater volume of supratentorial white matter  
<sup>24</sup> hyperintensities is associated with less time spent in functional MRI-derived brain  
<sup>25</sup> states of high fractional occupancy; and b) that less time spent in these high-occupancy  
<sup>26</sup> brain states is associated with longer time to completion in part B of the TMT.

<sup>27</sup> 

---

## <sup>28</sup> Introduction

<sup>29</sup> Cerebral small vessel disease (cSVD) is an arteriolopathy of the brain, associated with  
<sup>30</sup> age and common cardiovascular risk factors (Wardlaw, C. Smith, and Dichgans, 2013).  
<sup>31</sup> cSVD predisposes to ischemic, in particular lacunar, stroke and may lead to cognitive im-  
<sup>32</sup> pairment and dementia (Cannistraro et al., 2019). Neuroimaging findings in cSVD reflect  
<sup>33</sup> its underlying pathology (Wardlaw, Valdés Hernández, and Muñoz-Maniega, 2015) and  
<sup>34</sup> include white matter hyperintensities (WMH) and lacunes of presumed vascular origin,  
<sup>35</sup> small subcortical infarcts and microbleeds, enlarged perivascular spaces as well as brain  
<sup>36</sup> atrophy (Wardlaw, E. E. Smith, et al., 2013). However, the extent of visible cSVD features  
<sup>37</sup> on magnetic resonance imaging (MRI) is an imperfect predictor of the severity of clini-  
<sup>38</sup> cal sequelae (Das et al., 2019), and our understanding of the causal mechanisms linking  
<sup>39</sup> cSVD-associated brain damage to clinical deficits remains limited (Bos et al., 2018).

<sup>40</sup> Recent efforts have concentrated on exploiting network aspects of the structural (Tu-  
<sup>41</sup> ladhar, Dijk, et al., 2016; Tuladhar, Tay, et al., 2020; Lawrence, Zeestraten, et al., 2018) and  
<sup>42</sup> functional (Dey et al., 2016; Schulz et al., 2021) organization of the brain to understand  
<sup>43</sup> the relation between cSVD and clinical deficits in cognition and other domains reliant  
<sup>44</sup> on distributed processing. Reduced structural network efficiency has repeatedly been  
<sup>45</sup> described as a causal factor in the development of cognitive impairment, in particular

<sup>46</sup> executive dysfunction, in cSVD (Lawrence, Chung, et al., 2014; Shen et al., 2020; Reijmer  
<sup>47</sup> et al., 2016; Prins et al., 2005). Findings with respect to functional connectivity results, on  
<sup>48</sup> the other hand, are more heterogeneous, perhaps due to its limited reproducibility in  
<sup>49</sup> the presence of cSVD and dependence on arbitrary processing choices (Lawrence, Tozer,  
<sup>50</sup> et al., 2018; Gesierich et al., 2020). As a promising new avenue, time-varying, or dynamic,  
<sup>51</sup> functional connectivity approaches have more recently been explored in patients with  
<sup>52</sup> subcortical ischemic vascular disease (Yin et al., 2022; Xu et al., 2021).

<sup>53</sup> In the present paper, we aim to replicate and extend the main results of (Schlemm  
<sup>54</sup> et al., 2022); in this recent study, the authors analyzed MR imaging and clinical data from  
<sup>55</sup> the prospective Hamburg City Health Study (HCHS, (Jagodzinski et al., 2020)) using a coac-  
<sup>56</sup> tivation pattern approach to define discrete brain states and found associations between  
<sup>57</sup> the WMH load, time spent in high-occupancy brain states characterized by activation or  
<sup>58</sup> suppression of the default mode network (DMN) and executive dysfunction.

<sup>59</sup> Our primary hypothesis is that the volume of supratentorial white matter hyperinten-  
<sup>60</sup> sities is associated with the fractional occupancy (defined below) of DMN-related brain  
<sup>61</sup> states in a middle-aged to elderly population mildly affected by cSVD. Our second hypoth-  
<sup>62</sup> esis is that this fractional occupancy is associated with executive dysfunction, measured  
<sup>63</sup> as the time to complete part B of the trail making test (TMT).

<sup>64</sup> Both hypotheses will be tested in an independent subsample of the HCHS study popu-  
<sup>65</sup> lation using the same imaging protocols, examination procedures and analysis pipelines  
<sup>66</sup> as in (Schlemm et al., 2022). The robustness of associations will be explored in a multi-  
<sup>67</sup> verse approach by varying key steps in the analysis pipeline.

## <sup>68</sup> Methods

### <sup>69</sup> Study population

<sup>70</sup> The paper will analyze data from the Hamburg City Health Study (HCHS), which is an  
<sup>71</sup> ongoing prospective, population-based cohort study aiming to recruit a cross-sectional

<sup>72</sup> sample of 45 000 adult participants from the city of Hamburg, Germany (Jagodzinski et  
<sup>73</sup> al., 2020). From the first 10 000 participants of the HCHS we will aim to include those  
<sup>74</sup> who were documented to have received brain imaging (n=2652) and exclude those who  
<sup>75</sup> were analyzed in our previous report (Schlemm et al., 2022). The ethical review board of  
<sup>76</sup> the Landesärztekammer Hamburg (State of Hamburg Chamber of Medical Practitioners)  
<sup>77</sup> approved the HCHS (PV5131), all participants provided written informed consent.

## <sup>78</sup> **Demographic and clinical characterization**

<sup>79</sup> From the study database we will extract participants' age at the time of inclusion in years,  
<sup>80</sup> their self-reported gender and the number of years spent in education. During the visit  
<sup>81</sup> at the study center, participants undergo cognitive assessment using standardized tests.  
<sup>82</sup> We will extract from the database their performance scores in the Trail Making Test part B,  
<sup>83</sup> measured in seconds, as an operationalization of executive function (Tombaugh, 2004).

## <sup>84</sup> **MRI acquisition and preprocessing**

<sup>85</sup> The magnetic resonance imaging protocol for the HCHS includes structural and resting-  
<sup>86</sup> state functional sequences. The acquisition parameters on a 3 T Siemens Skyra MRI scan-  
<sup>87</sup> ner (Siemens, Erlangen, Germany) have been reported before (Petersen et al., 2020; Frey  
<sup>88</sup> et al., 2021) and are given as follows:

<sup>89</sup> For  $T_1$ -weighted anatomical images, a 3D rapid acquisition gradient-echo sequence  
<sup>90</sup> (MPRAGE) was used with the following sequence parameters: repetition time TR = 2500 ms,  
<sup>91</sup> echo time TE = 2.12 ms, 256 axial slices, slice thickness ST = 0.94 mm, and in-plane resolu-  
<sup>92</sup> tion IPR =  $(0.83 \times 0.83) \text{ mm}^2$ .

<sup>93</sup>  $T_2$ -weighted fluid attenuated inversion recovery (FLAIR) images were acquired with  
<sup>94</sup> the following sequence parameters: TR = 4700 ms, TE = 392 ms, 192 axial slices, ST =  
<sup>95</sup> 0.9 mm, IPR =  $(0.75 \times 0.75) \text{ mm}^2$ .

<sup>96</sup> 125 resting state functional MRI volumes were acquired (TR = 2500 ms; TE = 25 ms;  
<sup>97</sup> flip angle = 90°; slices = 49; ST = 3 mm; slice gap = 0 mm; IPR =  $(2.66 \times 2.66) \text{ mm}^2$ ). Subjects  
<sup>98</sup> were asked to keep their eyes open and to think of nothing.

<sup>99</sup> We will verify the presence and voxel-dimensions of expected MRI data for each par-  
<sup>100</sup> ticipant and exclude those for whom at least one of  $T_1$ -weighted, FLAIR and resting-state  
<sup>101</sup> MRI is missing. To ensure reproducibility, no visual quality assessment on raw images  
<sup>102</sup> will be performed.

<sup>103</sup> For the remaining participants, structural and resting-state functional MRI data will  
<sup>104</sup> be preprocessed using FreeSurfer v6.0 (<https://surfer.nmr.mgh.harvard.edu/>), and fmriPrep  
<sup>105</sup> v20.2.6 (Esteban et al., 2019), using default parameters. Participants will be excluded if  
<sup>106</sup> automated processing using at least one of these packages fails.

## <sup>107</sup> **Quantification of WMH load**

<sup>108</sup> For our primary analysis, the extent of ischemic white matter disease will be operational-  
<sup>109</sup> ized as the total volume of supratentorial WMHs obtained from automated segmentation  
<sup>110</sup> using a combination of anatomical priors, BIANCA (Griffanti, Zamboni, et al., 2016) and  
<sup>111</sup> LOCATE (Sundaresan et al., 2019), post-processed with a minimum cluster size of 30 vox-  
<sup>112</sup> els, as described in (Schlemm et al., 2022). In an exploratory analysis, we partition voxels  
<sup>113</sup> identified as WMH into deep and periventricular components according to their distance  
<sup>114</sup> to the ventricular system (cut-off 10 mm, (Griffanti, Jenkinson, et al., 2018))

## <sup>115</sup> **Brain state estimation**

<sup>116</sup> Output from fMRIprep will be post-processed using xcpEngine v1.2.1 to obtain de-confounded  
<sup>117</sup> spatially averaged BOLD time series (Circi, Wolf, et al., 2017). For the primary analysis we  
<sup>118</sup> will use the  $36p$  regression strategy and the Schaefer-400 parcellation (Schaefer et al.,  
<sup>119</sup> 2018), as in (Schlemm et al., 2022).

<sup>120</sup> Different atlases and confound regression strategies, as implemented in xcpEngine,  
<sup>121</sup> will be included in the exploratory multiverse analysis.

<sup>122</sup> Co-activation pattern (CAP) analysis will be performed by first aggregating parcellated,  
<sup>123</sup> de-confounded BOLD signals into a  $(n_{\text{parcels}} \times \sum_i n_{\text{time points},i})$  feature matrix, where  $n_{\text{time points},i}$   
<sup>124</sup> denotes the number of retained volumes for subject  $i$  after confound regression. Cluster-  
<sup>125</sup> ing will be performed using the  $k$ -means algorithm ( $k = 5$ ) with distance measure given

<sup>126</sup> by 1 minus the sample Pearson correlation between points, as implemented in Matlab  
<sup>127</sup> R2021a. We will estimate subject- and state-specific fractional occupancies, which are  
<sup>128</sup> defined as the proportion of BOLD volumes assigned to each brain state (Vidaurre et al.,  
<sup>129</sup> 2018). The two states with the highest average occupancy will be identified as the basis  
<sup>130</sup> for further analysis.

## <sup>131</sup> Statistical analysis

<sup>132</sup> For demographic (age, gender, years of education) and clinical (TMT-B) variables the num-  
<sup>133</sup> ber of missing records will be reported. For non-missing values, we will provide descrip-  
<sup>134</sup> tive summary statistics using median and interquartile range. The proportion of men  
<sup>135</sup> and women in the sample will be reported.

<sup>136</sup> As a first outcome-neutral quality check of the implementation of the MRI process-  
<sup>137</sup> ing pipeline, brain state estimation and co-activation pattern analysis, we will compare  
<sup>138</sup> fractional occupancies between brain states. We expect that the average fractional oc-  
<sup>139</sup> cupancy in two high-occupancy states is higher than the average fractional occupancy in  
<sup>140</sup> the other three states. Point estimates and 95% confidence intervals will be presented  
<sup>141</sup> for the difference in average fractional occupancy to check this assertion.

<sup>142</sup> For further analyses, non-zero WMH volumes will be subjected to a logarithmic trans-  
<sup>143</sup> formation. Zero values will retain their value zero; to compensate, all models will include  
<sup>144</sup> a binary indicator for zero WMH volume if at least one non-zero value is present.

<sup>145</sup> To assess the primary hypothesis of a negative association between the extent of is-  
<sup>146</sup> chemic white matter disease and time spent in high-occupancy brain states, we will per-  
<sup>147</sup> form a fixed-dispersion beta-regression to model the logit of the conditional expectation  
<sup>148</sup> of the average fractional occupancy of two high-occupancy states as an affine function of  
<sup>149</sup> the logarithmized WMH load. Age and gender will be included as covariates. The strength  
<sup>150</sup> of the association will be quantified as an odds ratio per interquartile ratio of the WMH  
<sup>151</sup> burden distribution and accompanied by a 95% confidence interval. Significance testing  
<sup>152</sup> of the null hypothesis of no association will be conducted at the conventional significance

<sup>153</sup> level of 0.05. Estimation and testing will be carried out using the 'betareg' package v3.1.4  
<sup>154</sup> in R v4.2.1.

<sup>155</sup> To assess the secondary hypothesis of an association between time spent in high-  
<sup>156</sup> occupancy brain states and executive dysfunction, we will perform a generalized linear  
<sup>157</sup> regression with a Gamma response distribution to model the logarithm of the condi-  
<sup>158</sup> tional expected completion time in part B of the TMT as an affine function of the average  
<sup>159</sup> fractional occupancy of two high-occupancy states. Age, gender, years of education and  
<sup>160</sup> logarithmized WMH load will be included as covariates. The strength of the association  
<sup>161</sup> will be quantified as a multiplicative factor per percentage point and accompanied by a  
<sup>162</sup> 95% confidence interval. Significance testing of the null hypothesis of no association will  
<sup>163</sup> be conducted at the conventional significance level of 0.05. Estimation and testing will  
<sup>164</sup> be carried out using the glm function included in the 'stats' package from R v4.2.1.

<sup>165</sup> Sample size calculation is based on the data presented in (Schlemm et al., 2022),  
<sup>166</sup> where an odds ratio of 0.95 was reported as the primary effect size of interest. We used  
<sup>167</sup> simple bootstrapping to create 10 000 hypothetical datasets of size 200, 400, 600, 800, 900,  
<sup>168</sup> 910, ..., 1100, 1200, 1400, 1500, 1600. Each dataset was subjected to the estimation pro-  
<sup>169</sup> cedure described above. For each sample size, the proportion of datasets in which the  
<sup>170</sup> primary null hypothesis of no association between fractional occupancy and WMH load  
<sup>171</sup> could be rejected at  $\alpha = 0.05$  was computed and is recorded as a power curve in Figure 1.

<sup>172</sup> It is seen that a sample size of 960 would allow replication of the reported effect with  
<sup>173</sup> a power of 80.2 %. We anticipate a sample size of 1500, which yields a power of 93.9 %.

## <sup>174</sup> Multiverse analysis

<sup>175</sup> Both in (Schlemm et al., 2022) and for our primary replication analysis we made cer-  
<sup>176</sup> tain analytical choices in the operationalisation of brain states and ischemic white mat-  
<sup>177</sup> ter disease, namely the use of the 36p confound regression strategy, the Schaefer-400  
<sup>178</sup> parcellation and a BIANCA/LOCATE-based WMH segmentation algorithm. If the hypoth-  
<sup>179</sup> esized association between WMH burden and time spent in high-occupancy states can

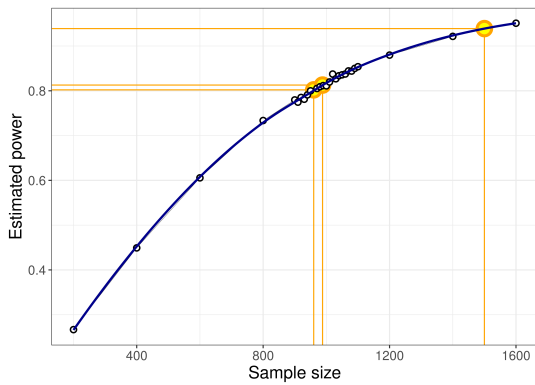


**Figure 1.** Estimated power for different sample sizes is obtained as the proportion of synthetic data sets in which the null hypothesis of no association between WMH volume and time spent in high-occupancy brain states can be rejected at the  $\alpha = 0.05$  significance level. Proportions are based on a total of 10 000 synthetic data sets obtained by bootstrapping the data presented in (Schlemm et al., 2022). Highlighted in orange are the smallest sample size ensuring a power of at least 80 % ( $n = 960$ ), the sample size of the pilot data ( $n = 988$ , post-hoc power 81.3 %), and the expected sample size for this replication study ( $n = 1500$ , a-priori power 93.9 %).

---

180 be replicated using these primary analytical choices, its robustness with regard to other  
 181 choices will be explored in a multiverse analysis (Schlemm et al., 2022; Steegen et al.,  
 182 2016). Specifically, we will estimate brain states from BOLD time series processed ac-  
 183 cording to a variety of established confound regression strategies and aggregated over  
 184 different cortical brain parcellations (Table 1, Ceric, Rosen, et al., 2018; Ceric, Wolf, et al.,  
 185 2017). Extent of cSVD will additionally be quantified by the volume of deep and periven-  
 186 tricular white matter hyperintensities.

187 For each combination of analytical choice of confound regression strategy, parcella-  
 188 tion and subdivision of white matter lesion load ( $9 \times 9 \times 3 = 243$  scenarios in total) we will  
 189 quantify the association between WMH load and average time spent in high-occupancy  
 190 brain states using odds ratio and 95 % confidence intervals as described above. No hy-  
 191 pothesis testing and, therefore, no adjustment for multiple testing, will be carried out in  
 192 these non-primary analyses.

Name of the atlas	#parcels	Reference	Design	Reference
Desikan-Killiany	86	Desikan et al., 2006	24p	Friston et al., 1996
AAL	116	Tzourio-Mazoyer et al., 2002	24p + GSR	Macey et al., 2004
Harvard-Oxford	112	Makris et al., 2006	36p	Satterthwaite et al., 2013
glasser360	360	Glasser et al., 2016	26p + spike regression	Cox, 1996
gordon333	333	Gordon et al., 2016	36p + despiking	Satterthwaite et al., 2013
power264	264	Power, Cohen, et al., 2011	36p + scrubbing	Power, Mitra, et al., 2014
schaefer{N}	100	Schaefer et al., 2018	aCompCor	Muschelli et al., 2014
	200		tCompCor	Behzadi et al., 2007
	400		AROMA	Pruim et al., 2015

AAL: Automatic Anatomical Labelling

(a) Parcellations

GSR: Global signal regression, AROMA: bla

(b) Confound regression strategies, adapted from (Ciric, Wolf, et al., 2017)

**Table 1.** Multiverse analysis, implemented using xcpEngine (Ciric, Rosen, et al., 2018)

## Exploratory analysis

In previous work, two high-occupancy brain states were related to the default-mode network (Cornblath et al., 2020). We will further explore this relation by computing, for each individual brain state, the cosine similarity of the positive and negative activations of the cluster's centroid with a set of a-priori defined functional 'communities' or networks (Schaefer et al., 2018; Yeo et al., 2011). Results will be thus visualized as spider plots for the Schaefer, Gordon and Power atlases.

## Code and pilot data

Summary data from the first 1000 imaging data points of the HCHS have been published with (Schlemm et al., 2022) and form the basis for the hypotheses tested in this replication study. We have implemented our prespecified analysis pipeline described above in R and Matlab, and applied it to this previous sample. Data, code and results have been stored on GitHub ([https://github.com/csi-hamburg/HCHS\\_brain\\_states\\_RR](https://github.com/csi-hamburg/HCHS_brain_states_RR)) und preserved on Zenodo.

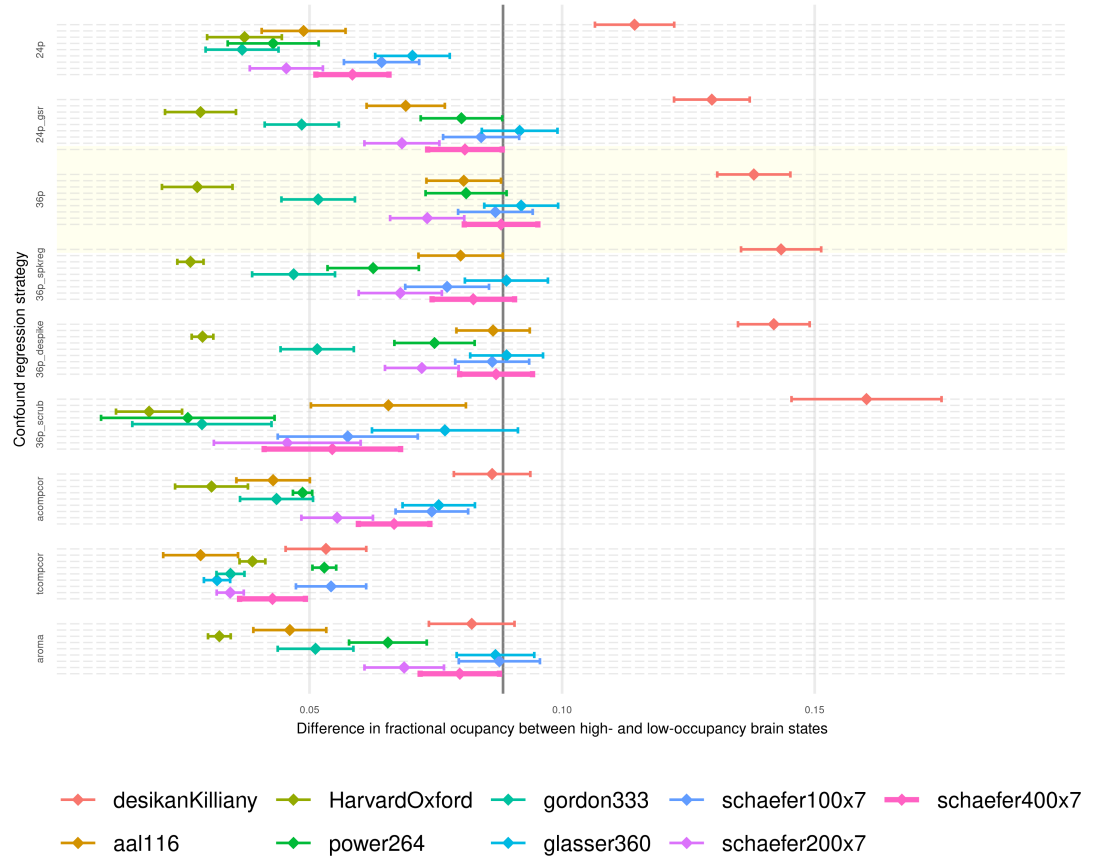


**Figure 2.** Point estimates and 95 % confidence intervals for the mean in fractional occupancy between high- and low occupancy states are shown for different confound regression strategies and brain parcellations. The primary choices (*36p* and *schaefer400*) are highlighted by a yellow box and thick pink line, respectively. The effect size reported in (Schlemm et al., 2022) is indicated by a vertical line at 0.08830623.

207 Thus re-analysing data from 988 subjects, the separation between two high-occupancy  
 208 and three low-occupancy brain states could be reproduced for all combinations of brain  
 209 parcellation and confound regression strategies (Figure 2).

210 In a multiverse analysis, the main finding was somewhat robust with respect to these  
 211 choices: a statistically significant negative association between WMH load and time spent  
 212 in high-occupancy states was observed in 18/81 scenarios, with 5/81 statistically signifi-  
 213 cant positive associations occurring with the Desikan–Killiany parcellation only (Figure 3).

214 The secondary finding of an association between greater TMT-B times and lower frac-

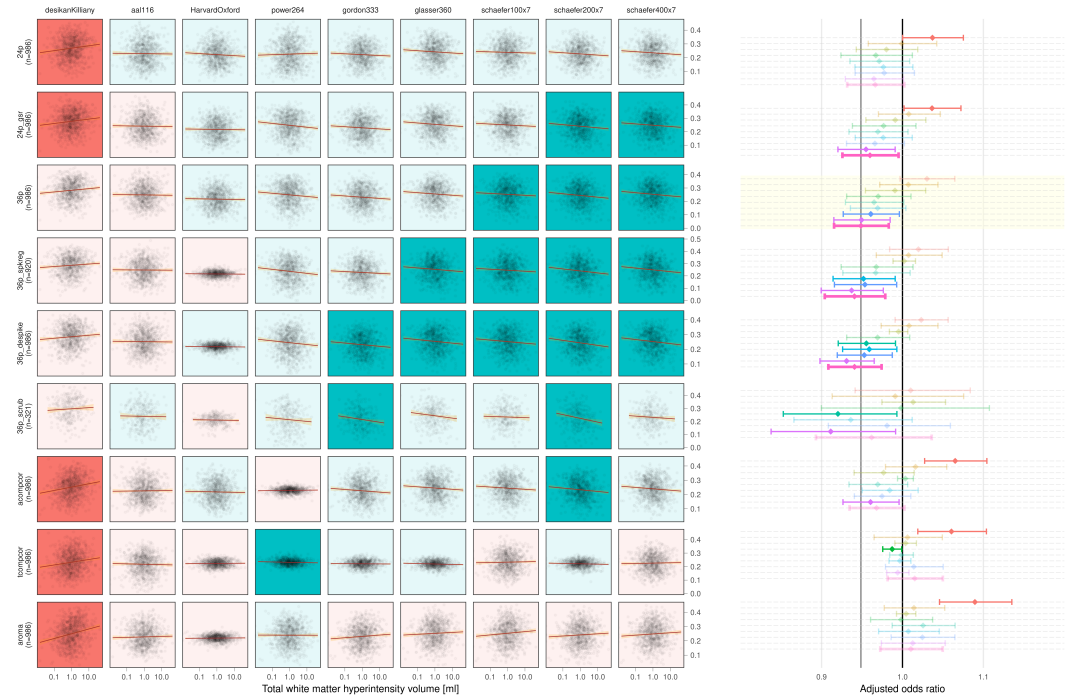


**Figure 3.** On the left, scatter plots of average fractional occupancies in high-occupancy states against WMH volume on a logarithmic scale (base 10 for easier visualization) for different combinations of confound regression strategies and brain parcellations. Linear regression lines indicate the direction of the unadjusted association between  $\log(\text{WMH})$  and occupancy. Background color of individual panels indicates the direction of the association after adjustment for age, sex and zero WMH volume (green, negative; red, positive). A pale background indicates that the association between  $\log(\text{WMH})$  and average occupancy is not statistically different from zero. On the right, the same information is shown using point estimates and 95 % confidence intervals for the adjusted odds ratio of the association.

<sup>215</sup> tional occupancy was similarly robust with 12/81 statistically significant negative and no  
<sup>216</sup> statistically significant positive associations.

## <sup>217</sup> **Timeline and access to data**

<sup>218</sup> At the time of planning of this study, all demographic, clinical and imaging data used in  
<sup>219</sup> this analysis have been collected by the HCHS and are held in the central trial database.  
<sup>220</sup> Quality checks for non-imaging variables have been performed centrally. WMH segmen-  
<sup>221</sup> tation based on structural MRI data of the first 10 000 participants of the HCHS has been  
<sup>222</sup> performed previously using the BIANCA/LOCATE approach (Rimmele et al., 2022) and re-  
<sup>223</sup> sults are included in this preregistration (./derivatives/WMH/cSVD\_all.csv). Functional  
<sup>224</sup> MRI data and clinical measures of executive dysfunction (TMT-B scores) have not been  
<sup>225</sup> analyzed by the author. Analysis of the data will begin immediately after acceptance-in-  
<sup>226</sup> principle of the stage 1 submission of the registered report is obtained. Submission of  
<sup>227</sup> the full manuscript (stage 2) is planned two months later.

## <sup>228</sup> **Acknowledgment**

<sup>229</sup> This preprint was created using the LaPreprint template ([https://github.com/roaldarbol/](https://github.com/roaldarbol/lapreprint)  
<sup>230</sup> [lapreprint](#)) by Mikkel Roald-Arbøl .

## <sup>231</sup> **References**

- <sup>232</sup> Behzadi, Yashar et al. (2007). "A component based noise correction method (CompCor)  
<sup>233</sup> for BOLD and perfusion based fMRI". In: *Neuroimage* 37.1, pp. 90–101.
- <sup>234</sup> Bos, Daniel et al. (2018). "Cerebral small vessel disease and the risk of dementia: A sys-  
<sup>235</sup> tematic review and meta-analysis of population-based evidence". en. In: *Alzheimers.*  
<sup>236</sup> *Dement.* 14.11, pp. 1482–1492.
- <sup>237</sup> Cannistraro, Rocco J et al. (2019). "CNS small vessel disease: A clinical review". en. In: *Neu-*  
<sup>238</sup> *rology* 92.24, pp. 1146–1156.

- <sup>239</sup> Ceric, Rastko, Adon FG Rosen, et al. (2018). "Mitigating head motion artifact in functional  
<sup>240</sup> connectivity MRI". In: *Nature protocols* 13.12, pp. 2801–2826.
- <sup>241</sup> Ceric, Rastko, Daniel H Wolf, et al. (2017). "Benchmarking of participant-level confound  
<sup>242</sup> regression strategies for the control of motion artifact in studies of functional con-  
<sup>243</sup> nectivity". en. In: *Neuroimage* 154, pp. 174–187.
- <sup>244</sup> Cornblath, Eli J et al. (2020). "Temporal sequences of brain activity at rest are constrained  
<sup>245</sup> by white matter structure and modulated by cognitive demands". en. In: *Commun Biol*  
<sup>246</sup> 3.1, p. 261.
- <sup>247</sup> Cox, Robert W (1996). "AFNI: software for analysis and visualization of functional mag-  
<sup>248</sup> netic resonance neuroimages". In: *Computers and Biomedical research* 29.3, pp. 162–  
<sup>249</sup> 173.
- <sup>250</sup> Das, Alvin S et al. (2019). "Asymptomatic Cerebral Small Vessel Disease: Insights from  
<sup>251</sup> Population-Based Studies". en. In: *J. Stroke Cerebrovasc. Dis.* 21.2, pp. 121–138.
- <sup>252</sup> Desikan, Rahul S et al. (2006). "An automated labeling system for subdividing the human  
<sup>253</sup> cerebral cortex on MRI scans into gyral based regions of interest". In: *Neuroimage* 31.3,  
<sup>254</sup> pp. 968–980.
- <sup>255</sup> Dey, Ayan K et al. (2016). "Pathoconnectomics of cognitive impairment in small vessel  
<sup>256</sup> disease: A systematic review". en. In: *Alzheimers. Dement.* 12.7, pp. 831–845.
- <sup>257</sup> Esteban, Oscar et al. (2019). "fMRIPrep: a robust preprocessing pipeline for functional  
<sup>258</sup> MRI". en. In: *Nat. Methods* 16.1, pp. 111–116.
- <sup>259</sup> Frey, Benedikt M et al. (2021). "White matter integrity and structural brain network topol-  
<sup>260</sup> ogy in cerebral small vessel disease: The Hamburg city health study". en. In: *Hum. Brain  
Mapp.* 42.5, pp. 1406–1415.
- <sup>262</sup> Friston, Karl J et al. (1996). "Movement-related effects in fMRI time-series". In: *Magnetic  
resonance in medicine* 35.3, pp. 346–355.
- <sup>264</sup> Gesierich, Benno et al. (2020). "Alterations and test-retest reliability of functional connec-  
<sup>265</sup> tivity network measures in cerebral small vessel disease". en. In: *Hum. Brain Mapp.*  
<sup>266</sup> 41.10, pp. 2629–2641.

- <sup>267</sup> Glasser, Matthew F et al. (2016). "A multi-modal parcellation of human cerebral cortex".  
<sup>268</sup> en. In: *Nature* 536.7615, pp. 171–178.
- <sup>269</sup> Gordon, Evan M et al. (2016). "Generation and Evaluation of a Cortical Area Parcellation  
<sup>270</sup> from Resting-State Correlations". en. In: *Cereb. Cortex* 26.1, pp. 288–303.
- <sup>271</sup> Griffanti, Ludovica, Mark Jenkinson, et al. (2018). "Classification and characterization of  
<sup>272</sup> periventricular and deep white matter hyperintensities on MRI: A study in older adults".  
<sup>273</sup> en. In: *Neuroimage* 170, pp. 174–181.
- <sup>274</sup> Griffanti, Ludovica, Giovanna Zamboni, et al. (2016). "BIANCA (Brain Intensity AbNormal-  
<sup>275</sup> ity Classification Algorithm): A new tool for automated segmentation of white matter  
<sup>276</sup> hyperintensities". en. In: *Neuroimage* 141, pp. 191–205.
- <sup>277</sup> Jagodzinski, Annika et al. (2020). "Rationale and Design of the Hamburg City Health Study".  
<sup>278</sup> en. In: *Eur. J. Epidemiol.* 35.2, pp. 169–181.
- <sup>279</sup> Lawrence, Andrew J, Ai Wern Chung, et al. (2014). "Structural network efficiency is as-  
<sup>280</sup> sociated with cognitive impairment in small-vessel disease". en. In: *Neurology* 83.4,  
<sup>281</sup> pp. 304–311.
- <sup>282</sup> Lawrence, Andrew J, Daniel J Tozer, et al. (2018). "A comparison of functional and trac-  
<sup>283</sup> tography based networks in cerebral small vessel disease". en. In: *Neuroimage Clin* 18,  
<sup>284</sup> pp. 425–432.
- <sup>285</sup> Lawrence, Andrew J, Eva A Zeestraten, et al. (2018). "Longitudinal decline in structural  
<sup>286</sup> networks predicts dementia in cerebral small vessel disease". en. In: *Neurology* 90.21,  
<sup>287</sup> e1898–e1910.
- <sup>288</sup> Macey, Paul M et al. (2004). "A method for removal of global effects from fMRI time series".  
<sup>289</sup> In: *Neuroimage* 22.1, pp. 360–366.
- <sup>290</sup> Makris, Nikos et al. (2006). "Decreased volume of left and total anterior insular lobule in  
<sup>291</sup> schizophrenia". In: *Schizophrenia research* 83.2-3, pp. 155–171.
- <sup>292</sup> Muschelli, John et al. (2014). "Reduction of motion-related artifacts in resting state fMRI  
<sup>293</sup> using aCompCor". In: *Neuroimage* 96, pp. 22–35.

- <sup>294</sup> Petersen, Marvin et al. (2020). "Network Localisation of White Matter Damage in Cerebral  
<sup>295</sup> Small Vessel Disease". en. In: *Sci. Rep.* 10.1, p. 9210.
- <sup>296</sup> Power, Jonathan D, Alexander L Cohen, et al. (2011). "Functional network organization of  
<sup>297</sup> the human brain". en. In: *Neuron* 72.4, pp. 665–678.
- <sup>298</sup> Power, Jonathan D, Anish Mitra, et al. (2014). "Methods to detect, characterize, and re-  
<sup>299</sup> move motion artifact in resting state fMRI". In: *Neuroimage* 84, pp. 320–341.
- <sup>300</sup> Prins, Niels D et al. (2005). "Cerebral small-vessel disease and decline in information pro-  
<sup>301</sup> cessing speed, executive function and memory". en. In: *Brain* 128.Pt 9, pp. 2034–2041.
- <sup>302</sup> Pruim, Raimon HR et al. (2015). "ICA-AROMA: A robust ICA-based strategy for removing  
<sup>303</sup> motion artifacts from fMRI data". In: *Neuroimage* 112, pp. 267–277.
- <sup>304</sup> Reijmer, Yael D et al. (2016). "Small vessel disease and cognitive impairment: The rele-  
<sup>305</sup> vance of central network connections". en. In: *Hum. Brain Mapp.* 37.7, pp. 2446–2454.
- <sup>306</sup> Rimmele, David Leander et al. (2022). "Association of Carotid Plaque and Flow Velocity  
<sup>307</sup> With White Matter Integrity in a Middle-aged to Elderly Population". en. In: *Neurology*.
- <sup>308</sup> Satterthwaite, Theodore D et al. (2013). "An improved framework for confound regres-  
<sup>309</sup> sion and filtering for control of motion artifact in the preprocessing of resting-state  
<sup>310</sup> functional connectivity data". In: *Neuroimage* 64, pp. 240–256.
- <sup>311</sup> Schaefer, Alexander et al. (2018). "Local-Global Parcellation of the Human Cerebral Cortex  
<sup>312</sup> from Intrinsic Functional Connectivity MRI". en. In: *Cereb. Cortex* 28.9, pp. 3095–3114.
- <sup>313</sup> Schlemm, Eckhard et al. (2022). "Equalization of Brain State Occupancy Accompanies  
<sup>314</sup> Cognitive Impairment in Cerebral Small Vessel Disease". en. In: *Biol. Psychiatry* 92.7,  
<sup>315</sup> pp. 592–602.
- <sup>316</sup> Schulz, Maximilian et al. (2021). "Functional connectivity changes in cerebral small vessel  
<sup>317</sup> disease - a systematic review of the resting-state MRI literature". en. In: *BMC Med.* 19.1,  
<sup>318</sup> p. 103.
- <sup>319</sup> Shen, Jun et al. (2020). "Network Efficiency Mediates the Relationship Between Vascular  
<sup>320</sup> Burden and Cognitive Impairment: A Diffusion Tensor Imaging Study in UK Biobank".  
<sup>321</sup> en. In: *Stroke* 51.6, pp. 1682–1689.

- <sup>322</sup> Steegen, Sara et al. (2016). "Increasing Transparency Through a Multiverse Analysis". en.  
<sup>323</sup> In: *Perspect. Psychol. Sci.* 11.5, pp. 702–712.
- <sup>324</sup> Sundaresan, Vaanathi et al. (2019). "Automated lesion segmentation with BIANCA: Im-  
<sup>325</sup> pact of population-level features, classification algorithm and locally adaptive thresh-  
<sup>326</sup> olding". en. In: *Neuroimage* 202, p. 116056.
- <sup>327</sup> Tombaugh, Tom N (2004). "Trail Making Test A and B: normative data stratified by age  
<sup>328</sup> and education". en. In: *Arch. Clin. Neuropsychol.* 19.2, pp. 203–214.
- <sup>329</sup> Tuladhar, Anil M, Ewoud van Dijk, et al. (2016). "Structural network connectivity and cog-  
<sup>330</sup> nition in cerebral small vessel disease". en. In: *Hum. Brain Mapp.* 37.1, pp. 300–310.
- <sup>331</sup> Tuladhar, Anil M, Jonathan Tay, et al. (2020). "Structural network changes in cerebral small  
<sup>332</sup> vessel disease". en. In: *J. Neurol. Neurosurg. Psychiatry* 91.2, pp. 196–203.
- <sup>333</sup> Tzourio-Mazoyer, Nathalie et al. (2002). "Automated anatomical labeling of activations in  
<sup>334</sup> SPM using a macroscopic anatomical parcellation of the MNI MRI single-subject brain".  
<sup>335</sup> In: *Neuroimage* 15.1, pp. 273–289.
- <sup>336</sup> Vidaurre, Diego et al. (2018). "Discovering dynamic brain networks from big data in rest  
<sup>337</sup> and task". en. In: *Neuroimage* 180.Pt B, pp. 646–656.
- <sup>338</sup> Wardlaw, Joanna M, Colin Smith, and Martin Dichgans (2013). "Mechanisms of sporadic  
<sup>339</sup> cerebral small vessel disease: insights from neuroimaging". en. In: *Lancet Neurol.* 12.5,  
<sup>340</sup> pp. 483–497.
- <sup>341</sup> Wardlaw, Joanna M, Eric E Smith, et al. (2013). "Neuroimaging standards for research  
<sup>342</sup> into small vessel disease and its contribution to ageing and neurodegeneration". en.  
<sup>343</sup> In: *Lancet Neurol.* 12.8, pp. 822–838.
- <sup>344</sup> Wardlaw, Joanna M, María C Valdés Hernández, and Susana Muñoz-Maniega (2015). "What  
<sup>345</sup> are white matter hyperintensities made of? Relevance to vascular cognitive impair-  
<sup>346</sup> ment". en. In: *J. Am. Heart Assoc.* 4.6, p. 001140.
- <sup>347</sup> Xu, Yuanhang et al. (2021). "Altered Dynamic Functional Connectivity in Subcortical Is-  
<sup>348</sup> chemic Vascular Disease With Cognitive Impairment". en. In: *Front. Aging Neurosci.* 13,  
<sup>349</sup> p. 758137.

- <sup>350</sup> Yeo, B T Thomas et al. (2011). "The organization of the human cerebral cortex estimated  
<sup>351</sup> by intrinsic functional connectivity". en. In: *J. Neurophysiol.* 106.3, pp. 1125–1165.
- <sup>352</sup> Yin, Wenwen et al. (2022). "The Clustering Analysis of Time Properties in Patients With  
<sup>353</sup> Cerebral Small Vessel Disease: A Dynamic Connectivity Study". en. In: *Front. Neurol.*  
<sup>354</sup> 13, p. 913241.